Eur Biophys J (2012) 41:107–114
DOI 10.1007/s00249-011-0775-3

ORIGINAL PAPER

Understanding UV-driven metabolism in the hypersaline ciliate *Fabrea salina*

Roberto Marangoni · Debora Paris · Dominique Melck · Lorenzo Fulgentini · Giuliano Colombetti · Andrea Motta

Received: 11 March 2011 / Revised: 26 October 2011 / Accepted: 31 October 2011 / Published online: 18 November 2011

Abstract By using NMR spectroscopy, a non-invasive investigation technique, we performed in vivo experiments aimed at uncovering the metabolic pathways involved in the early response of *Fabrea salina* cells to ultraviolet (UV) radiation. This hypersaline ciliate was chosen as a model organism because of its well-known high resistance to UV radiation. Identical cell samples were exposed to visible radiation only (control samples, CS) and to UV-B + UV-A + visible radiation (treated samples, TS), and NMR spectra of in vivo cells were collected at different exposure times. Resonances were identified through one- and two-dimensional experiments. To compare experiments performed at variable irradiation times on different culture batches, metabolite signals affected by the UV exposure were normalized to corresponding intensity at $\tau = 0$, the zero exposure time. The most affected metabolites are all osmoprotectants, namely, choline, glycine-betaine, betaines, ectoine, proline, α-trehalose and sucrose. The time course of these signals presents qualitative differences between CS and TS, and most of these osmoprotectants tend to accumulate significantly in TS in a UV dose-dependent manner. A picture of the immediate stress response of *F. salina* against UV radiation in terms of osmoprotection, water retention and salting-out prevention is described.

Keywords *Fabrea salina* · NMR · Osmoprotectant · Metabolomics · Hypersaline

Abbreviations

NMR	Nuclear magnetic resonance
UV	Ultraviolet
CS	Control samples
TS	Treated samples

Roberto Marangoni, Debora Paris and Dominique Melck contributed equally to this work.

Special Issue: SIBPA 2011 Meeting.

R. Marangoni (✉)
Dipartimento di Informatica, Università di Pisa, Pisa, Italy
e-mail: marangon@di.unipi.it

R. Marangoni · L. Fulgentini · G. Colombetti
Istituto di Biofisica del CNR, Pisa, Italy

D. Paris · D. Melck · A. Motta
Istituto di Chimica Biomolecolare del CNR, Pozzuoli, NA, Italy

Introduction

It is well known that exposure of living matter to ultraviolet (UV) radiation can cause a broad variety of damages: photochemical alterations of nucleic acids and proteins, often mediated by active oxygen species and free radicals (Caldwell et al. 1998), formation of cyclobutane pyrimidine dimers in the DNA (Brash 1997), and biochemical and physiological processes such as reduction in mRNA synthesis, decreased enzyme production (Kumar et al. 1996; Sinha et al. 1996, 1998), long-term biological consequences like morphogenetic aberrations, and impaired growth and restricted mobility (Kennedy 1995). In plants, a partial inhibition of photosynthesis is also observed (Caldwell et al. 1998). In ecological communities, UV radiation alters the equilibrium by compromising the survival of less-resistant species and favoring the more resistant ones (Häder et al. 1998; Marangoni et al. 2004). One of the major concerns regards the stability of marine ecosystems, which are the most important producers of organic matter on our planet (Häder 2004). UV-B radiation (280–315 nm) can deeply penetrate along the water column (Malloy et al. 1997; Hargreaves 2003), therefore affecting photosynthetic and non-photosynthetic marine organisms with significant DNA damage and reduction of the photosynthetic rate. This results in a decrease in primary productivity, which, in turn, negatively influences all trophic levels in the food chain (Melis et al. 1992; Sinha et al. 2004). Moreover, the reduced photosynthetic activity contributes to increasing the greenhouse effect by reducing the total ocean CO_2 absorption, thus establishing a strong link between different global climate changes (Häder et al. 2007a).

To reduce the impact of UV-induced damages, marine organisms have developed several repair and attenuation mechanisms, such as blue light and UV-A (315–400 nm) activated DNA repair processes (Buma et al. 1996; Sinha et al. 2004), storage of protecting agents like carotenoids and detoxifying enzymes (Middleton and Teramura 1993), and the de novo production of mycosporine-like amino acids (MAAs) or other photo-protective compounds (Sinha et al. 1999; Adams and Shick 2008) and light-avoidance motility behavior (Spudich and Spudich 2008).

UV effects at the ecological level have recently been investigated by applying some of the modern "omics" approaches, like genomics and proteomics, which have respectively assessed the genes and the proteins that are affected by UV exposure. Among omic sciences, metabolomics studies the complete set of metabolites/low-molecular-weight intermediates, which are context dependent and vary according to the physiology, developmental or pathological state of the cell, tissue, organ or organisms (Oliver et al. 2002; Harrigan and Goodacre 2003; Lindon et al. 2006; Griffiths 2007). In particular, environmental metabolomics characterizes the interactions of living organisms with the environment, aiming at understanding organismal responses to abiotic stressors, including both natural (i.e., temperature or UV-B radiation) and anthropogenic (i.e., pollution) factors (Lois 1994; Day et al. 2001; Broeckling et al. 2005; Bundy et al. 2009).

Here we focus on the moderate halophile ciliate *Fabrea salina* (optimal growth at 5–16% NaCl) for two main reasons. First, although it has an important role in the stability of the ocean's ecosystems, playing a prominent role in aquatic food webs as a trophic link between phytoplankton and metazoan zooplankton, only a few reports deal with the effect of UV radiation on *F. salina* (Marangoni et al. 2004). Second, this extremophile shows a well-known strong resistance to UV radiation (Moeller 1962), suggesting that the molecular devices involved in sensing and reacting against UV are very efficient and, per se, have potentially valuable applications.

It has been demonstrated that UV irradiation (in particular, UV-B) causes a transient increase of cell speed and a progressive decrease of positive phototaxis (Martini et al. 1997). We have recently reported (Marangoni et al. 2011) that NMR-based metabolomics of in vivo *F. salina* cells is able to successfully investigate UV-induced alteration of metabolic profiles. We analyzed: (1) control samples (CS) exposed to visible light (Vis) and (2) treated samples (TS) exposed to polychromatic radiation ranging from UV-B to Vis at increasing irradiation time exposures. Multivariate data analysis based on in vivo NMR spectra showed differences in metabolic profiles of CS with respect to TS. Principal component analysis (PCA) revealed different trends and clusters in the samples, and clearly indicated UV-induced dose-dependent signals. We successfully identified two clusters of signals that appeared to be specifically induced by UV irradiation, characterized by a different lifetime. The first cluster, the earliest and most transient, included acetate and formate, and was interpreted as a stress indicator. Their NMR signals increased immediately after the first minutes of irradiation, returning to a basal value after 15 min, when the system was probably recovering from stress. The second cluster contained several metabolites, almost all of which were osmoprotectants, whose signals appeared to be UV dose-dependent and did not disappear for the entire duration of the experiments. This cluster was interpreted as the most interesting pathway of UV response, most likely induced by UV-operated membrane poration that turns a radiative stress into an osmotic one.

To better characterize such UV-induced late response of *F. salina* cells, we herein specifically focused on the second cluster of metabolites. To safely compare different batches of *F. salina* cells, concentration variations of metabolites affected by UV exposure at variable irradiation time were estimated by normalizing to the intensity at zero exposure time and quantified. Through relative quantification of metabolite concentration, we suggest that an increase of osmoprotectant concentration during the experiment time proves that the first target of UV radiation most likely is the cell membrane.

Materials and methods

F. salina cultures

Cells of the halophile heterotrichous ciliate *F. salina*, originating from a strain collected ca. 6 years ago from a salt marsh in Torre Colimena (TA, Italy), were cultivated in sterilized artificial sea water (salinity of 76‰) and fed with the microalgae *Dunaliella salina* grown at the same water temperature and illumination cycle used for

F. salina. All cultures were subjected to a light/dark cycle of 15-h light and 9-h dark, the light sources being two fluorescent lamps emitting in the Vis (Philips TLD 30 W/54, Royal Philips Electronics, Amsterdam, The Netherlands). *F. salina* cells were starved for 2 days before the experiments and collected by filtration with filters of 30-µm pore size (permeable to *D. salina*) to rule out any possible algal contamination.

Irradiation protocol

In order to irradiate the samples as close as possible to the NMR spectrometer, a home-made mobile irradiation apparatus was built. It was equipped with six lamps, four emitting in the UV (Philips PL-S 9W/12/2P 1CT, Royal Philips Electronics, Amsterdam, The Netherlands) and two emitting in the Vis (Philips PL-S 2P 9W/840, Royal Philips Electronics, Amsterdam, The Netherlands). This setup allows the switch on all six lamps or only the Vis-emitting ones. The spectra of both irradiation regimes were measured using a calibrated ORIEL INSTANSPEC IV radiometric spectrograph (LOT-Oriel Europe, Milan, Italy), and the results are reported in Fig. 1. In Table 1 the total irradiances supplied in the two irradiation regimes are compared with the environmental values derived from Eldonet Database (Häder et al. 2007b). The UV-B emitting lamps are clearly able to efficiently cover the UV-A spectral band, generating a polychromatic irradiation that mimics a UV-B-enriched solar spectrum.

In each experiment cells were collected and concentrated by filtration, and randomly divided into two identical samples that counted about 40,000 cells each. They were put in quartz cuvettes (usually employed for optical fluorescence measurements) that are fully transparent to actinic

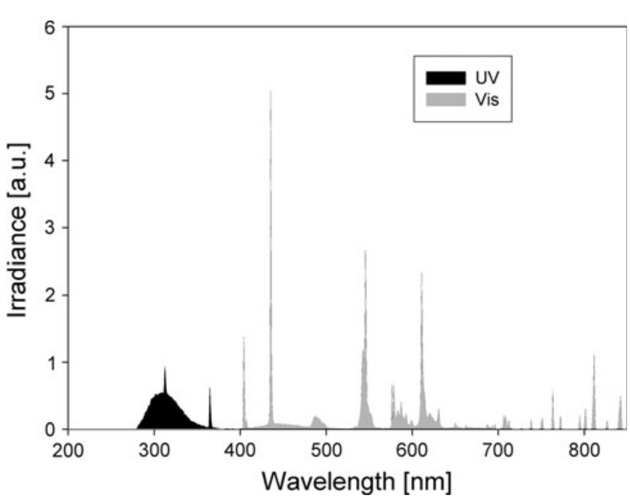

Fig. 1 Emission spectra for the UV and Vis irradiation regimes. In *black* the area covered by UV lamps, in *gray* the area covered by the visible lamps

Table 1 Irradiance values for the three main spectral bands for treated (exposed to regime 1) and control (exposed to regime 2) samples

Spectral band	Regime 1 (UV-B + UV-A + Vis) irradiance values (W/m^2)	Regime 2 (Vis) irradiance values (W/m^2)	Environmental values (average range) (W/m^2)
Vis	78.09	51.79	400–420
UV-A	9.85	0.04	50–55
UV-B	16.13	0.00	1.0–1.3
UV-B/UV-A	1.64	0.00	0.018–0.026

Environmental values, reported as reference, are derived from the Eldonet database (Häder et al. 2007b)

radiation. Control samples (CS) were exposed to only the visible component of the radiation, while treated samples (TS) were exposed to the entire spectrum (UV-B + UV-A + Vis). NMR spectra of TS samples were recorded at $\tau = 7$, 15, 22, 30, 37, 45 and 60 min of total irradiation, while CS samples were sampled every 15 min, as CS showed a less variable trend. Experiments were in quadruplicate, using a different cell culture each time. CS and TS of the same culture batch were run in parallel and processed with exactly the same protocol, the only difference being the spectrum of the actinic radiation. During irradiation and spectrum acquisition, the temperature was kept constant at 23°C.

NMR sample preparation

After irradiation, 630 µl of each *F. salina* sample was rapidly transferred to an NMR tube, adding 70 µl of a D_2O solution [containing 0.1 mM sodium 3-trimethylsilyl (2,2,3,3-$^2H_4$) propionate (TSP) as an internal chemical shift reference for ^1H spectra and 3-mM sodium azide] to provide a field frequency lock, therefore reaching a total volume of 700 µl.

NMR measurements

All spectra were recorded on a 600-MHz Bruker Avance spectrometer (Bruker BioSpin GmbH, Rheinstetten, Germany) equipped with a CryoProbe™ fitted with a gradient along the *Z*-axis. One-dimensional (1D) ^1H-NMR spectra were collected at 300 K with the excitation sculpting pulse sequence (Hwang and Shaka 1995) to suppress the water resonance. We used a double-pulsed field gradient echo with a soft square pulse of 4 ms at the water resonance frequency, with the gradient pulses of 1 ms each in duration, adding 128 transients of 65,536 complex points, with a spectral width of 7,002.8 Hz. Time-domain data were all zero-filled to 131,072 complex points, and prior to Fourier transformation an exponential multiplication of 0.6 Hz was applied. Two-dimensional (2D) NMR spectra [namely, ^{1}H–^{1}H clean total correlation spectroscopy (TOCSY) and natural abundance ^{1}H–^{13}C heteronuclear single quantum coherence (HSQC)] were acquired and processed as reported (Marangoni et al. 2011). 1D and 2D TOCSY spectra were referred to the TSP signal, assumed to resonate at $\delta = 0.00$ ppm; 2D HSQC spectra were referred to the alanine βCH_3 signal, assumed to resonate at 1.49 ppm for ^{1}H and 16.80 ppm for ^{13}C.

Signals intensity sampling and time course monitoring

We have previously identified many of the signals present in the NMR spectra of *F. salina* (Marangoni et al. 2011). Furthermore, by means of principal component analysis (PCA), a specific set of signals was recognized as significantly related to UV radiation exposure. Here we focus on the most significant ones, namely choline, glycine betaine/β-alanine betaine, betaines, ectoine, proline, sucrose and α-trehalose, whose chemical shifts are listed in Table 2. In order to be able to compare different experiments and avoid the large variations of the absolute values, the intensity of each signal was obtained from each sampling and normalized against the value at the beginning of each experiment ($\tau = 0$).

Table 2 ^{1}H and ^{13}C chemical shift assignments (δ, ppm) of the selected metabolites for *F. salina* (labeled according to Marangoni et al. 2011)

Entry	Metabolite	δ ^{1}H	δ ^{13}C	Group
12	Proline	2.01	23.40	γCH_2
		2.08	29.10	$\beta' CH$
		2.36	29.10	βCH
		3.29	44.90	δCH
		3.45	44.90	$\delta' CH$
		4.09	61.04	αCH
13	Ectoine	2.25	18.95	CH_3
18	Choline moiety	3.21	51.35	NCH_3
		4.03	53.26	αCH_2
19	Betaines	3.25	55.86	$N(CH_3)_3$
		3.89	68.64	NCH_2
20	Glycine betaine/	3.28	53.84	NCH_3
	β-alanine betaine	3.93	66.29	$\alpha CH_2/\beta CH_2$
22	α-Trehalose	3.42	69.46	C4H
		3.58	71.20	C5H
		3.73	72.85	C3H
		3.75; 3.85	60.12	C6H
		86	72.40	C2H
		5.24	94.65	C1H
23	Sucrose	3.43	72.40	G4H
		3.65	62.00	F1H
		3.85	63.20	F6H
		3.98	74.43	F4H
		5.40	92.87	G1H

Results and discussion

Figure 2 depicts a typical homonuclear TOCSY spectrum (Fig. 2a) and the corresponding heteronuclear HSQC spectrum (Fig. 2b) of in vivo *F. salina* cells, UV-irradiated for 37 min. The spectra allowed the identification of the ^{1}H–^{1}H (TOCSY) and the directly bonded ^{1}H–^{13}C (HSQC) correlations, and the proton and carbon assignments of the discussed metabolites are reported in Table 2. We acquired 1D and 2D spectra of TS samples at τ = 7, 15, 22, 30, 37,

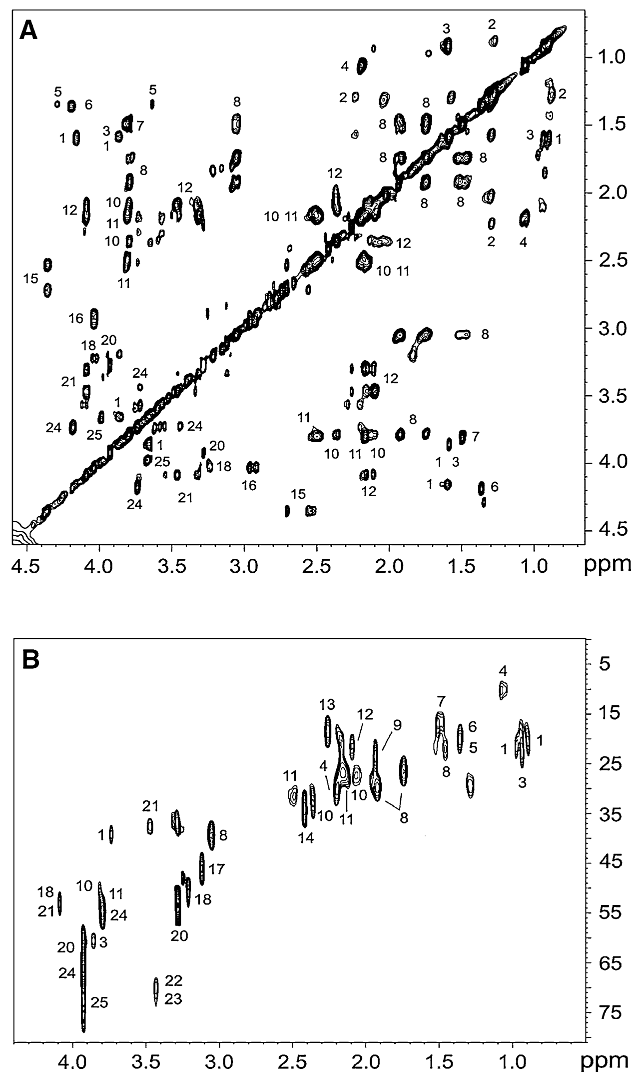

Fig. 2 In-vivo 2D spectra of *F. salina* cells irradiated with UV for 37 min. **a** TOCSY and **b** HSQC. Cross peaks are labeled according to the assignments reported in Marangoni et al. (2011)

45 and 60 min of total irradiation and corresponding CS samples. Within experimental errors, the spectra well reproduce those already reported (Marangoni et al. 2011), confirming the reproducibility of the approach.

Choline signal time course

The time course of choline signal is similar in both CS and TS, showing a decreasing trend that reaches a plateau after 30 min of total exposure time (Fig. 3), but with TS significantly lower than CS. The choline CS variation is of unknown origin and does not appear to be linked to osmoprotection activity, especially when compared with the time course of glycine-betaine (Fig. 4), which slightly decreases in CS. In higher organisms, choline participates in a large number of reactions. Besides the transformation of choline in glycine-betaine, the two main ones are the syntheses of phosphatidylcholine (essential for the cell membrane) and of acetylcholine, which has not been proved to exist in *F. salina*. The most reasonable explanation for the observed decrease in CS is a normal synthetic activity for the cell membrane maintenance. On the contrary, the more accentuated decreasing trend in TS suggests an osmoprotection activity, as the decrease in choline is a premise for the increase in glycine-betaine (Fig. 4), which derives from it and is a more effective osmoprotectant.

Glycine-betaine signal time course

In CS glycine-betaine shows a slow decreasing trend, with ca. 50% reduction after 1 h of total irradiation time

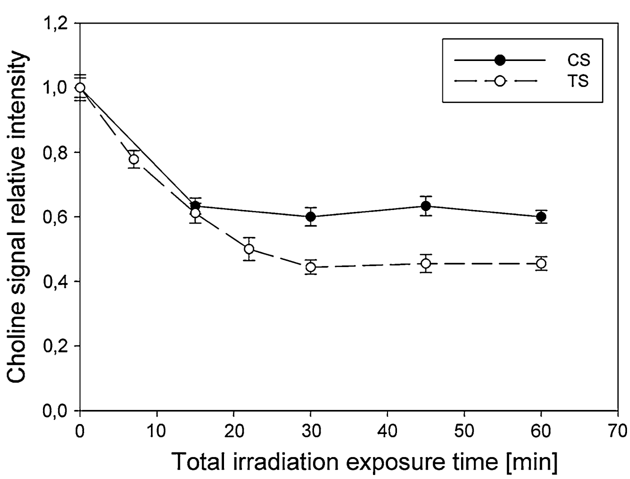

Fig. 3 Choline moieties time course for CS (*solid line*, *filled circles*) and TS (*dashed line*, *empty circles*). Abscissa: the total exposure time (min); ordinate: the signal intensity for choline, normalized in all the samples against its value at $\tau = 0$. The *error bar* refers to the standard error of the mean

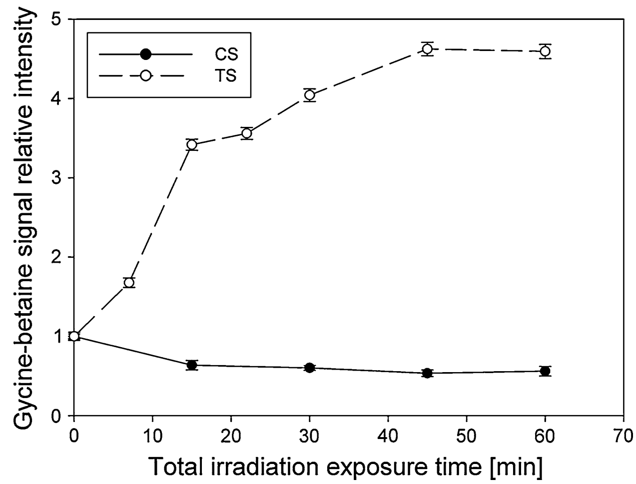

Fig. 4 Glicine-betaine time course for CS and TS. *Symbols* and *notations* are the same of Fig. 2

(Fig. 4). On the contrary, in TS it shows a strong increase beyond 400% of the initial intensity after 45 min of total exposure to UV radiation. Glycine-betaine is usually employed in cells as a homocysteine detox agent, and therefore its decrease in CS could be linked to a normal cell function. On the contrary, the strong increase in TS suggests a required osmoprotectant function, with glycine-betaine being one of the most effective protectants for cell membranes (Jolivet et al. 1982; Mansur 1998). On the other hand, glycine-betaine/β-alanine betaine, besides the osmoregulating function, stabilizes the oxygen evolution activity of the photosystem protein complex (Yeo 1998) in photosynthetic organisms. TS also shows an increase in alanine (data not shown), which is probably involved in the production of the β-alanine betaine through its mehtylation (McNeil et al. 1999) via *N*-methyl and *N*,*N*-dimethyl β-alanines. As stated above, the observed decrease of choline moieties for TS (Fig. 3) is consistent with the synthesis of glycine betaine via oxidation, which increases for cumulative UV radiation (Fig. 4).

Betaines signal time course

The NMR signals stemming from betaines different from glycine-betaines/β-alanine betaine and proline-betaine are all grouped in an unresolved broad signal (see Table 2). The behavior of this signal is difficult to understand as its time course in CS is about constant, while it shows a strong up-and-down oscillation in TS (Fig. 5) with a decreasing average trend. Although the main role of betaines is in osmoregulation, they are also used as an energy source during periods of prolonged stress (Riou et al. 1991). Therefore, the observed zigzagging variation could be related to an on–off energy requirement. From the above

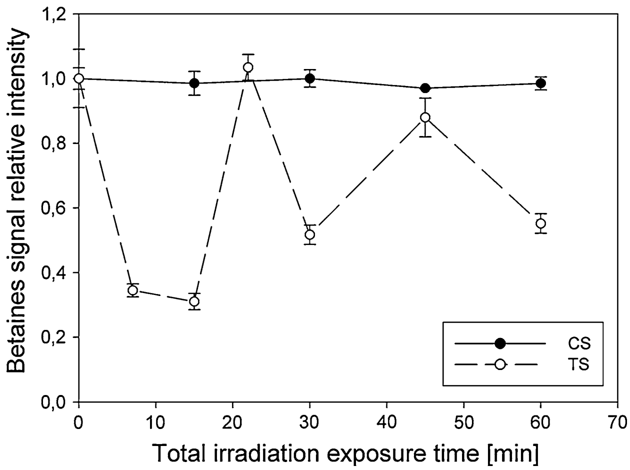

Fig. 5 Betaines time course for CS and TS. *Symbols* and *notations* are the same of Fig. 2

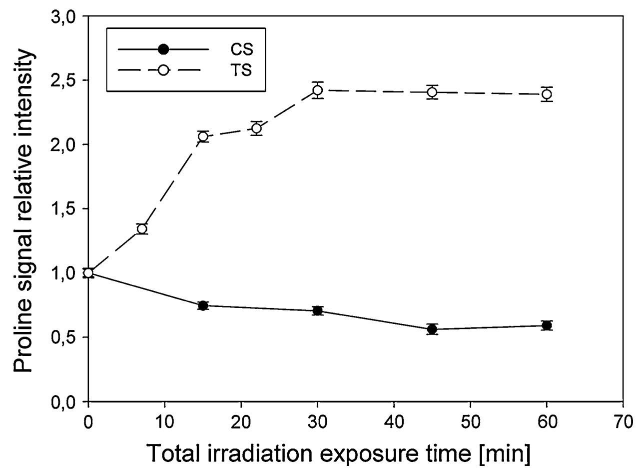

Fig. 7 Proline time course for CS and TS. *Symbols* and *notations* are the same as in Fig. 2

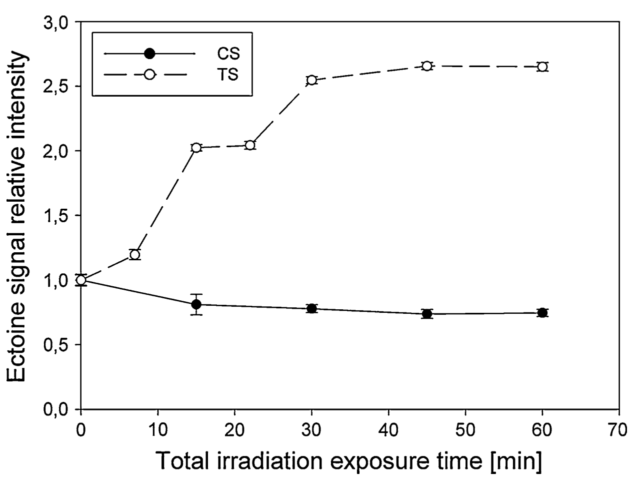

Fig. 6 Ectoine time course for CS and TS. *Symbols* and *notations* are the same as in Fig. 2

considerations, we can hypothesize that betaines act as a source for other osmoconformers (e.g., glycine-betaine/β-alanine betaine, proline) to supply additive osmoprotection in the UV-induced stress conditions.

Ectoine signal time course

The ectoine signal time course (Fig. 6) is qualitatively similar to that of glycin-betaine (Fig. 4): decreasing in CS and increasing in TS, albeit this is quantitatively less evident. The substantially opposite behavior of betaines and ectoine (Figs. 5, 6) could be interpreted as a switch in osmolyte buildup, since betaines accumulate in high proportions with low cytoplasmatic NaCl and ectoine at a high concentration of cytoplasmatic NaCl (Da Costa et al. 1998). Ectoine helps salt-tolerant organisms in highly saline environments and slows the diffusion of water through the cell membrane, allowing the single-cell organisms to maintain the proper level of hydration.

Proline signal time course

The proline time course in CS and TS (Fig. 7) is very close to that of ectoine (Fig. 6) and glycine-betaine (Fig. 4), as it accumulates in TS and decreases in CS (Fig. 7). Proline has an important role in osmoregulation. In different stress conditions it holds multiple key functions such as formation of the carbon and nitrogen source, protection of enzyme denaturation, regulation of cytoplasmic acidity and detoxification of cells from free radicals (Alia et al. 1993; Delauney and Verma 1993; Naqvi et al. 1997). Therefore, the strong accumulation in TS plays a clear anti-stress protection role.

α-Trehalose and sucrose

While they remain about constant in CS, α-trehalose and sucrose slightly decrease in TS (data not shown). This trend could be ascribed to the protective effect against the water leakage caused by the UV-induced membrane poration. Indeed, the principal role of α-trehalose is to allow the cell to survive under anhydrous conditions, with the sugar being able to form a gel that prevents the development of damage to intracytoplasmic organelles and preserves them in vital condition (Iturriaga et al. 2009).

Conclusions

We have demonstrated that changes in the metabolism of *F. salina* cells after UV irradiation can be efficiently investigated by in vivo NMR spectroscopy. Resonance identification and detection of changes in the intensity of some important osmoprotectants prove that the first cellular reaction to radiation damage consists of a general accumulation of osmoprotectants and anti-stress molecules. This strongly suggests that the first target of UV radiation (or the first revealed target) is the cell membrane. We are currently investigating the second-level response of *F. salina* upon UV irradiation, which is activated soon after this “emergency call.”

References

Adams NL, Shick JM (2008) Mycosporine-like amino acids provide protection against ultraviolet radiation in eggs of the green sea urchin *Strongylocentrotus droebachiensis*. Photochem Photobiol 64:149–158

Alia S, Saradhi PP, Mohanty P (1993) Proline in relation to free radical production in seedlings of *Brassica juncea* raised under sodium chloride stress. Plant Soil 155(156):497–500

Brash DE (1997) Sunlight and the onset of skin cancer. Trend Genet 13:410–414

Broeckling CD, Huhman DV, Farag MA, Smith JT, May GD, Mendes P et al (2005) Metabolic profiling of *Medicago truncatula* cell cultures reveals the effects of biotic and abiotic elicitors on metabolism. J Exp Botany 56:323–336

Buma AGJ, van Hannen EJ, Veldhuis MJW, Gieskes WWC (1996) UV-B induces DNA damage and DNA synthesis delay in the marine diatom *Cyclotella* sp. Sci Mar 60:101–105

Bundy JG, Matthew PD, Viant MR (2009) Environmental metabolomics: a critical review and future perspectives. Metabolomics 5:3–21

Caldwell MM, Björn LO, Bornman JF, Flint SD, Kulandaivelu G, Teramura AH, Tevini M (1998) Effects of increased solar ultraviolet radiation on terrestrial ecosystems. J Photochem Photobiol B (Biol) 46:40–52

Da Costa MS, Santos H, Galinski EA (1998) An overview of the role and diversity of compatible solutes in bacteria and archaea. Adv Biochem Bioeng/Biotechnol 61:117–158

Day TAC, Ruhland T, Xiong FS (2001) Influence of solar ultraviolet-B radiation on Antarctic terrestrial plants: results from a 4-year field study. J Photochem Photobiol B (Biol) 62:78–87

Delauney AJ, Verma DPS (1993) Proline biosynthesis and osmoregulation in plants. Plant J 4:215–223

Griffiths W (2007) Metabolomics, metabonomics and metabolites profiling. The Royal Society of Chemistry, Cambridge

Häder DP (2004) Penetration and effects of solar UV-B on phytoplankton and macroalgae. Plant Ecol 128:5–13

Häder DP, Kumar HD, Smith RC, Worrest RC (1998) Effects on aquatic ecosystems. J Photochem Photobiol B (Biol) 46:53–68

Häder DP, Kumar HD, Smith RC, Worrest RC (2007a) Effects of solar UV radiation on aquatic ecosystems and interactions with climate change. Photochem Photobiol Sci 6:267–285

Häder DP, Lebert M, Schuster M, del Ciampo L, Helbling LW, McKenzie R (2007b) ELDONET—a decade of monitoring solar radiation on five continents. Photochem Photobiol 83:1348–1357

Hargreaves BR (2003) Water column optics and penetration of UVR. In: Helbling EW, Zagarese HE (eds) UV effects in aquatic organisms and ecosystems. The Royal Society of Chemistry, Cambridge

Harrigan GG, Goodacre R (2003) Metabolic profiling: its role in biomarker discovery and gene function analysis. Springer, Boston

Hwang TL, Shaka AJ (1995) Water suppression that works: excitation sculpting using arbitrary waveforms and pulse field gradients. J Magn Reson 112:275–279

Iturriaga G, Suárez R, Nova-Franco B (2009) Trehalose metabolism: from osmoprotection to signaling. Int J Mol Sci 10:3793–3810

Jolivet Y, Larher F, Hamelin J (1982) Osmoregulation in halophytic higher plants: the protective effect of glycine betaine against the heat destabilization of membranes. Plant Sci 25:193–201

Kennedy AD (1995) Antarctic terrestrial ecosystem response to global environmental change. Annu Rev Ecol Syst 26:683–704

Kumar A, Sinha RP, Häder DP (1996) Effect of UV-B on enzymes of nitrogen metabolism in the cyanobacterium *Nostoc calcicola*. J Plant Physiol 148:86–91

Lindon JC, Nicholson JK, Holmes E (2006) The handbook of metabonomics and metabolomics. Elsevier Science, London

Lois R (1994) Accumulation of UV-absorbing flavonoids induced by UV-B radiation in *Arabidopsis thaliana*.1. Mechanisms of UV-resistance in *Arabidopsis*. Planta 194:498–503

Malloy KD, Holman MA, Mitchell D, Detrich HW III (1997) Solar UVB-induced DNA damage and photoenzymatic DNA repair in Antarctic zooplankton. Proc Natl Acad Sci USA 94:1258–1263

Mansur MMF (1998) Protection of plasma membrane of onion epidermal cells by glycinbetaine and proline against NaCl stress. Plant Physiol Biochem 36:767–772

Marangoni R, Messina N, Gioffré D, Colombetti G (2004) Effects of UV-B irradiation on a marine microecosystem. Photochem Photobiol 80:78–83

Marangoni R, Paris D, Melck D, Fulgentini L, Colombetti G, Motta A (2011) In vivo NMR metabolic profiling of *Fabrea salina* reveals sequential defense mechanisms against UV. Biophys J 100:215–224

Martini B, Marangoni R, Gioffré D, Colombetti G (1997) Effect of UV-B irradiation on motility and photomotility of the marine ciliate *Fabrea salina*. J Photochem Photobiol B (Biol) 39:197–205

McNeil SD, Nuccio ML, Hanson AD (1999) Betaines and related osmoprotectant. Targets for metabolic engineering of stress resistence. Plant Physiol 120:945–949

Melis A, Nemson JA, Harrison NA (1992) Damage to functional components and partial degradation of Photosystem II reaction center proteins upon chloroplast exposure to ultraviolet-B radiation. Biochim Biophys Acta 1100:312–320

Middleton EM, Teramura AH (1993) The role of flavonol glycosides and carotenoids in protecting soybean from ultraviolet-B damage. Plant Physiol 103:741–752

Moeller KM (1962) On the nature of stentorin. Compt Rend Lab Carlsberg 32:471–498

Naqvi SSM, Mumtaz S, Shereen A, Khan MA, Khan AH (1997) Role of abscitic acid in regulation of wheat seedling growth under salinity stress. Biologia Plantarium 39:453–456

Oliver DJ, Nikolau B, Wurtele ES (2002) Functional genomics: high-throughput mRNA, protein, and metabolite analyses. Metab Eng 4:98–106

Riou N, Poggi MC, Le Rudulier D (1991) Characterization of an osmoregulated periplasmic glycine betaine-binding protein in *Azospirillum brasilense* sp7. Biochimie 71:1187–1193

Sinha RP, Singh N, Kumar A, Kumar HD, Häder M, Häder DP (1996) Effects of UV irradiation on certain physiological and biochemical processes in cyanobacteria. J Photochem Photobiol B (Biol) 32:107–113

Sinha RP, Klisch M, Gröniger A, Häder DP (1998) Ultraviolet-absorbing/screening substances in cyanobacteria, phytoplankton and macroalgae. J Photochem Photobiol B (Biol) 47:83–94

Sinha RP, Klisch M, Häder DP (1999) Induction of a mycosporine-like amino acid (MAA) in the rice-field cyanobacterium *Anabaena* sp. by UV irradiation. J Photochem Photobiol B (Biol) 52:59–64

Sinha RP, Klisch M, Gröniger A, Häder DP (2004) Responses of aquatic algae and cyanobacteria to solar UV-B. Plant Ecol 154:219–236

Spudich JL, Spudich EN (2008) The simplest eyes: rhodopsin-mediated phototaxis reception in microorganisms. In: Tsonis PA (ed) Animal models in eye research. Elsevier, Amsterdam, pp 6–14

Yeo A (1998) Molecular biology of salt tolerance in the context of whole-plant physiology. J Exp Bot 49:915–929